ACOUSTICS 2012

# A semi-empirical model to predict the acoustic behaviour of fully and partially reticulated polyurethane foams based on microstructure properties

O. Doutres and N. Atalla

Groupe d'Acoustique de l'Université de Sherbrooke, 2500 Boulevard de l'Université, Faculté de Génie, Sherbrooke, AB, Canada J1K2R1 QC
olivier.doutres@usherbrooke.ca

This work investigates the links between the microstructure of polyurethane foams and their sound absorbing efficiency, and more specifically the effect of membranes closing the cells. In a previous work, the authors proposed a semi-empirical approach to link the foam microstructure properties, i.e. reticulation rate, strut length and thickness, with its non-acoustic parameters. The study was based on the complete characterization of 15 isotropic polyurethane foams with various cell sizes and reticulation rates (i.e. open pore content). This paper proposes a validation of this semi-empirical model using 3 new polyurethane foams, not used in the first characterization set. More importantly, a simplification is presented to account only for the foam cell size and reticulation rate. Non-acoustic parameters estimated by the micro/macro links are also compared to direct and indirect measurements. It is shown that the proposed expressions associated to the Johnson-Champoux-Allard porous model allow for a good estimation of the sound absorbing behaviour of all tested polyurethane foams, fully reticulated or not.

# 1 Introduction

This work investigates the influence of the cell size and the reticulation rate of the porous microstructure on the acoustic behaviour of polyurethane (PU) foams. First, the links established previously by the authors [1] between microstructure properties of PU foams (i.e., cell shape, open pore content, strut length and thickness) and non-acoustic macroscopic parameters (i.e., porosity, airflow resistivity...) are presented. These links were developed using a semi-empirical approach based on 15 polyurethane foams whose typical microstructure is show in Figure 1. These 15 foams mainly vary by their cell size and closed pore content. According to this figure, the polyurethane foam microstructure can be seen as a collection of interlinked struts forming 3-D structures as a packing of tetrakaidecahedra cells. Each cell is connected to others through pores. Materials with 100% open pores are called "fully reticulated". In this case the interconnectivity between cells is optimal. If some of the pores are closed or partially closed by thin membranes, the material is called "partially reticulated". The semi-empirical approach proposed in [1] estimates the acoustic behaviour of PU foams from cell shape consideration and measurements of strut's length $l$, strut's thickness $t$ and reticulation rate $R_w$.

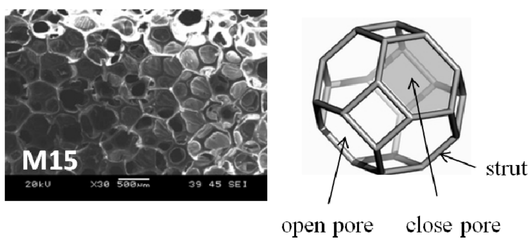


Figure 1: SEM picture of the partially reticulated polyurethane foam M15 and shape of the unit cell (PUC).

The aim of this paper is to validate this semi-empirical model using new polyurethane foams that have not been used in reference [1], that is in the derivation of the model. A simplification of this micro/macro semi-empirical model is also proposed to account only for cell size $C_s$ and reticulation rate $R_w$; measurements of strut length $l$ and thickness $t$ are no more required. Validation of the simplified micro/macro links is also proposed.

# 2 Foam characterization

## 2.1 Microstructure

Microstructure of the polyurethane foams is analysed from SEM pictures. As Perrot *et al.* [2] did in the case of open-cell aluminum foams, the microstructure of polyurethane foam is assumed as a packing of tetrakaidecahedra cells (see Figure 1) characterized by $f$=14 faces/cell and $n$=5.14 edges/face and independent of cell density. For each material, the properties of a representative tetrakaidecahedra unit-cell (also called PUC) from which the existing scaling laws would be applied are determined.

In this work, since we are interested in linking cell microstructure to non-acoustic parameters from simple models, only PU foams having isotropic cells are considered in the analysis. For each material, mean cell size of the unit-cell $C_s$ [μm], mean strut length $l$ [μm] and thickness $t$ [μm] are measured. The reticulation rate $R_w$ [%], which gives the open pore content of the material, is estimated from SEM images by the ratio of the number of open pore to the total number of pores. In reference [1], 15 materials were studied, 9 were fully reticulated ($R_w$=100%) and 6 partially reticulated with a reticulation rate ranging from 10% to 70%. The 15 isotropic polyurethane foams have cell sizes ranging from 500 μm to 1600 μm. It was observed that the strut thickness $t$, strut length $l$ and mean pore size increase linearly with cell size for both fully reticulated ($R_w$=100%) and partially reticulated materials ($R_w$<100%).

Also, it is found that the strut length to thickness ratio $l/t$ and the cell size to pore size ratio $C_s/W_m$ are almost identical for all cell sizes. This indicates that from one cell size to another, the shape of the cells is unchanged and their size parameters are only magnified by a given factor. Thus, in the case of PU foams, it is possible to find simple relations between strut dimensions and cell size. From all PU foam considered in this work it is found that the strut length $l$ is approximately equal to $l= C_s/A\sqrt{2}$, with $A$=2.33, which is very close to the theoretical value of $A$=2 for a tetrakaidecahedra isotropic unit cell, and the strut thickness $t$ is found to be equal to $t=l/B= C_s/AB\sqrt{2}$ with $B$=3.84. These scales factors are the basis of the model simplification proposed in this paper. Indeed, mean strut thickness and length can be simply deduced from measurement of the cell size. This simplifies the microstructure characterization and reduces the propagation of uncertainties in the measurement of the strut's thickness and length, to the estimation of the non-acoustic properties.

## 2.2 Non-acoustic properties

The non-acoustical parameters considered in this work are used in the Johnson-Champoux-Allard model to describe the visco-thermal and inertial couplings between the porous aggregate and the interstitial fluid on a macroscopic scale [3]: e.g. open porosity $\phi$, static air flow resistivity $\sigma$ [N.s/m$^4$], dynamic tortuosity $\alpha_\infty$, viscous $\Lambda$ [µm], and thermal characteristic lengths $\Lambda'$ [µm] and thermal static permeability $k_0'$ [m$^2$]. The porosity $\phi$ and the airflow resistivity $\sigma$ are measured using direct techniques [4][5]. For both fully and partially reticulated foams, the tortuosity $\alpha_\infty$ is estimated from indirect method based on ultrasound techniques. Tortuosity of fully reticulated materials is determined from ultrasonic measurement of transmitted waves [6]. This latter method being restricted to low resistive materials, the tortuosity $\alpha_\infty$ of partially reticulated foams is estimated from the measurement of acoustic waves reflected by a slab of porous material at oblique incidence [7]. The two characteristic lengths ($\Lambda$,$\Lambda'$) and the thermal permeability $k'_0$ are determined using the indirect characterization method proposed by Panneton and Olny [8][9]. This requires the measurement of the equivalent dynamic bulk modulus $K_{eq}$ and equivalent dynamic density $\rho_{eq}$ of the tested material performed here using the 3-microphone impedance tube method proposed by Salissou *et al.* [10]. The Lafarge *et al.* model [11] is used here to model the equivalent dynamic bulk modulus $K_{eq}$ because it was shown elsewhere to match more closely its low frequency behaviour [3]. This determination of the parameter $k'_0$ is mainly used here to lower the error in the determination of the thermal characteristic length $\Lambda'$. Indeed, since the thermal permeability parameter is not directly linked to microstructure geometry element or to another non-acoustic parameter, it will be discarded from the micro/macro analysis, at least for the time being.

# 3 Link microstructure and non-acoustic properties

This section briefly describes the micro/macro links presented in [1].

## 3.1 Porosity $\phi$, thermal length $\Lambda'$

Porosity $\phi$ and thermal characteristic length $\Lambda'$ of PU foams are determined from simple geometrical calculations based on the tetrakaidecahedra unit-cell shape assumption [1][2][12]. Porosity, defined as the ratio of the fluid volume $V_f$ to the total volume $V_t$, is given by

$$\phi = \frac{V_f}{V_t} = 1 - \frac{\rho_1}{\rho_s} = 1 - \rho_r \tag{1}$$

with $\rho_1$ the bulk density of the foam, $\rho_s$ the density of the strut material, and $\rho_r$ the relative density which can be expressed in terms of strut thickness $t$ and strut length $l$ forming the cells as $\rho_r$=$C^\rho(t/l)^2$. $C^\rho$ is a constant which depends on the microscopic geometrical properties of the foam, such as cell shape, strut cross section and joint region shape. In this case, struts are assumed to have a triangular concave cross-section shape and thus $C^\rho$ is equal to $(2\sqrt{3}-\pi)/\sqrt{2}$ [1]. Porosity of these highly porous open-cell foams does not depend on the cell size nor reticulation rate but only on the cell shape and ratio between strut length and thickness (i.e., $B$). Indeed, the effect of membranes is not taken into account here since the membrane volume can be neglected in the calculation of the frame volume $V_s$. Eq. (1) is used for partially reticulated polyurethane foams.

The thermal characteristic length $\Lambda'$ is defined as twice the average ratio of the cell volume $V_f$ to their wet surface $A_t$. It is thus possible to account for the effect of the thin membranes closing the cell pores on the wet surface $A_t$ such as

$$\Lambda' = \frac{2V_f}{A_t} = \frac{2V_f}{A_s + (1-R_w)A_w} \tag{2}$$

with $A_s$ the surface of the struts and $A_w$ the total surface of the pores weighted here by the closed pore rate (1-$R_w$), $R_w$ being the reticulation rate. $A_s$ can be calculated from the perimeter of the strut $P_s$ for a given cross-section shape. Assuming a tetrakaidecahedra unit cell, the surface of the 36 struts per cell $A_s$, is given by $A_s = 36lP_s/3$; the "1/3" coefficient accounts for the fact that one strut is shared between three cells. In this case, struts are assumed to have a triangular concave cross-section shape (as observed on SEM pictures) and $P_s$ is equal to $4\pi t/\sqrt{3}$. Note that the strut thickness $t$ is the height of the equilateral triangle with edge $a$ and concavity radius $R$=$a$. The total surface of the pores is determined from the total surface of the cell $A_c$ as $A_w = A_c - A_s$. For a tetrakaidecahedra unit cell, this surface is $A_c$=$(6+12\sqrt{3})l^2$. Note that for fully reticulated materials ($R_w$=100%), the wet surface area is only the surface of the struts $A_s$ and the thermal length of Eq. (2) reduces to the expression given by Perrot *et al.* [2] such as

$$\Lambda' = D_1 \frac{l^2}{t} - D_2 t \tag{3}$$

where $D_1$ and $D_2$ are numerical constants near unity which can be determined analytically for simple cases [1][2].

## 3.2 Viscous length $\Lambda$

In the case of fibrous materials, the viscous length can be predicted analytically from the calculation of the velocity field around a strut with circular cross-section shape, considering that the velocity far from the strut is perpendicular to the strut. In this case, the viscous characteristic length $\Lambda$ is related to the diameter $t$ of a fibre by [3]

$$\Lambda = \frac{t}{4\rho_r}. \tag{4}$$

This simple analytical model gives a good prediction of the viscous length for fully reticulated foams which thus can be considered having a fibrous-like behavior [1]. Using the same assumptions, Allard and Atalla [3] show that the thermal and viscous characteristic lengths of fibrous materials are linked by a factor 2 as $n$= $\Lambda'/\Lambda$=2 (when the macroscopic air velocity is perpendicular to the direction of the fibres). In the case of the fully reticulated polyurethane foam considered in [1] the ratio between the thermal and the viscous characteristic lengths ($n$=$\Lambda'/\Lambda$) is close to 1.55. Thus, the viscous length of fully reticulated PU foams can be derived from the geometrical estimation of the thermal length of Eq. (2) divided by $n$=1.55. Note that the viscous characteristic length $\Lambda$ may also be derived from the analytical study of the sound propagation in a pore channel and given by [3]

$$\Lambda = \frac{1}{c_g}\sqrt{\frac{8\eta\alpha_\infty}{\phi\sigma}}, \tag{5}$$

where $c_g$ is a pore shape dependent constant (it is equal to one for cylindrical pores) and $\eta$ is the viscosity of air ($\eta$=1.85e$^{-5}$). Eq. (5) is not used here since it requires the knowledge of the other inter-correlated non-acoustic parameters.

Presence of membranes closing the pores decreases the viscous characteristic length and increases the characteristic length ratio $n$ ($n=\Lambda'/\Lambda$) [1]. The constant relation between the two characteristic lengths found in the case of fully reticulated materials, i.e. $n$=1.55±0.2, can no longer be used for partially reticulated materials. Thus from the 6 partially reticulated materials used in [1], an empirical expression of the ratio $n$ is derived in terms of the closed pore content. It is given by

$$n=\frac{\Lambda'}{\Lambda}=1.55\left(\frac{1}{R_w}\right)^{0.676} . \qquad (6)$$

The viscous characteristic length $\Lambda$ for both fully and partially reticulated PU foams is obtained from Eqs. (2) and (6).

## 3.3 Airflow resistivity $\sigma$ and tortuosity $\alpha_\infty$

The scaling law proposed by Lind-Nordgren and Göransson [13][14] to link microstructure properties with the non-acoustic macroscopic airflow resistivity parameter is used and improved empirically to account for the presence of thin membranes closing the cell pores and inducing the partial reticulation

$$\sigma=\sigma'\left(\frac{1}{R_w}\right)^{1.116}=C^{\beta}\left(C^{\rho}\frac{t}{l^2}\right)^2\left(\frac{1}{R_w}\right)^{1.116} \qquad (7)$$

This scaling law, i.e. $\sigma'$=f($t$,$l$), combines different simplified models of wave propagation inside the microstructure and has a large number of implicit assumptions; propagation in a cylindrical pore ($c_g$=1 and validity of Eq. (5)), material with low tortuosity ($\alpha_\infty\approx1$) and high porosity ($\phi\approx$100%) and wave propagation perpendicular to ligament with a circular cross-section shape (validity of Eq. (4)). It is thus adapted to fully reticulated materials [1]. Note that in Eq. (7), $C^{\rho}$ is now associated to strut with circular cross-section shape ($C^{\rho}=3\pi/8\sqrt{2}$) because of the use of Eq. (4) and $C^{\beta}$ = $128\alpha_\infty\eta/c_g^2$ (note that $C^{\sigma}$ in [1] is changed for $C^{\beta}$ here to avoid any confusions with the airflow resistivity notation) with $\alpha_\infty$=$c_g$ =1. Still, Eq. (7) gives surprisingly a satisfactory prediction of the airflow resistivity for the nine studied fully reticulated polyurethane foams as shown in Figure 2 (compare blue circles with green triangles).

The tortuosity which has been found constant ($\alpha_\infty\approx$1.05) for highly porous and fully reticulated polyurethane foams, increases with the close pore content and is given empirically in [1] as

$$\alpha_\infty=1.05\left(\frac{1}{R_w}\right)^{0.380} . \qquad (8)$$

# 4 Model simplification

By using the two scale relations given at the end of section 2.1, the strut length and thickness required in Eqs. (1), (2) and (7) can be deduced from cell size measurement. This leads to a two parameters model: cell size and reticulation rate. For example, Eq. (7) can be rewritten as

$$\sigma=C^{\beta}\left(C^{\rho}\frac{A\sqrt{2}}{B}\right)^2\left(\frac{1}{C_s}\right)^2\left(\frac{1}{R_w}\right)^{1.116} . \qquad (9)$$

One can appreciate in Figure 2, that Eq. (9) associated to the cell size measurement provides a good estimate of the airflow resistivity of the 9 fully reticulated polyurethane foams measured by the authors [1] but also of the polyurethane foams measured by Lambert [15], Dunn and Davern [16] and Cummings and Beadle [17]. In addition, the inverse proportionality of the airflow resistivity with the square of the cell size, described in Eq.(9), agrees with both the empirical law provided by Cummings and Beadle (see Eq. (17.a) in [17]) for polyurethane foams and the experimental observations carried out by Bonnet *et al.* [18] on aluminum foams.

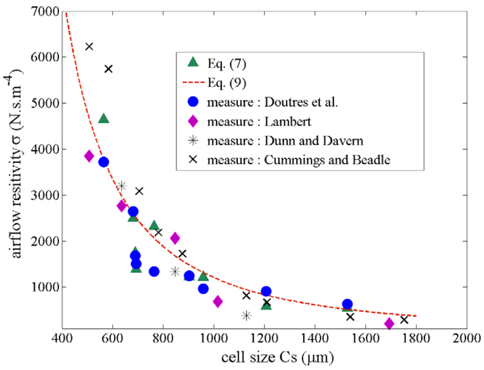


Figure 2: Airflow resistivity versus cell size for fully reticulated polyurethane foams ($R_w$=100%). Eq. (7) uses measurements of strut length and thickness; Eq. (9) uses measurement of cell size only.

# 5 Validation

To validate the proposed semi-empirical approach, three new isotropic polyurethane foams which have not been used during the development of the empirical model [1] are investigated. First, the microstructure properties are measured from SEM pictures as described in section 2.1. All non-acoustic properties are then estimated from Eqs. (1), (2), (6), (7) and (8) and compared to direct and indirect measurements as described in section 2.2. Finally, the sound absorption coefficients determined from the estimated non-acoustic properties, using the rigid equivalent fluid model, are compared to measurements performed in impedance tube according to standard ISO-10534-2 [19].

Microstructure properties of the three PU foams are given in Table 1. Foam P1 is a fully reticulated PU foam having the smallest cell size that can be produced. Foam P2 is partially reticulated foam with smallest cell size and a low reticulation rate. Foam P3 is partially reticulated foam with very large cell size and a very low reticulation rate. Table 2 and Table 3 give the non-acoustic properties estimated using Eqs. (1), (2), (6), (7) and (8) with strut length and thickness measurements or cell size measurements respectively. Table 4 presents the measured values which are considered here as reference values.

Table 1: Microstructure properties of three PU foams.

| foam | P1 | P2 | P3 |
|---|---|---|---|
| Mean cell size (μm) | 673 (±35) | 616 (±36) | 1710 (±161) |
| Mean strut length (μm) | 208 (±11) | 209 (±14) | 554 (±39) |
| Mean strut thickness (μm) | 46 (±4) | 50 (±11) | 151 (±8) |
| Reticulation rate (%) | 100 - | 32 (±11) | 5 (±2) |

Table 2: Non-acoustic properties of the three PU foams determined from the semi-empirical model associated to strut properties measurements ($l$ and $t$).

| foam | P1 | P2 | P3 |
|---|---|---|---|
| Porosity (%) | 98.8 | 98.7 | 98.3 |
| Airflow resistivity (kN.s.m$^{-4}$) | 1.9 | 7.8 | 10.5 |
| Tortuosity | 1.05 | 1.62 | 3.2 |
| Thermal length (μm) | 482 | 216 | 474 |
| Viscous length (μm) | 311 | 64 | 42 |

Table 3: Non-acoustic properties of the three PU foams determined from the semi-empirical model associated to measurement of cell size $C_s$.

| foam | P1 | P2 | P3 |
|---|---|---|---|
| Porosity (%) | 98.8 | 98.4 | 98.5 |
| Airflow resistivity (kN.s.m$^{-4}$) | 2.7 | 11.3 | 10.9 |
| Tortuosity | 1.05 | 1.62 | 3.2 |
| Thermal length (μm) | 402 | 191 | 445 |
| Viscous length (μm) | 259 | 57 | 39 |

Table 4: Non-acoustic properties of three PU foams measured according to section 2.2.

| foam | P1 | P2 | P3 |
|---|---|---|---|
| Porosity (%) | 95.9 | 95.7 | 97.1 |
| Airflow resistivity (kN.s.m$^{-4}$) | 3.5 | 17.4 | 19.4 |
| Tortuosity | 1.06 | 1.73 | 2.16 |
| Thermal length (μm) | 249 | 220 | 458 |
| Viscous length (μm) | 187 | 46 | 24 |

By comparing Tables 2, 3 and 4, it is shown that porosity is well estimated by the geometrical approach which validates the use of a tetrakaidecahedra unit-cell shape and struts having triangular concave cross-section shape. Airflow resistivity is underestimated by the semi-empirical model for the three foams. The discrepancies are however decreased by using the simplified model (see Tables 3 and 4). Note that this underestimation, which can be attributed to the simplicity of the scaling law of Eq. (7) and its numerous associated assumptions, nevertheless provides a satisfactory estimation of the sound absorption behavior as shown in Figure 3. Furthermore, one can note in Figure 2 that a large scattering in airflow resistivity measurement can also be observed for fully reticulated foam having small cell size inferior to 700 μm (compare foams with similar cell size measured by Doutres *et al.* [1], Lambert [15] and Cummings and Beadle [17]); which puts into perspective the underestimations provided by Eq. (7) for these three PU foams. The tortuosity values predicted by the semi-empirical model are in good agreements with measurements. Thermal and viscous characteristic lengths of the fully reticulated PU foam P1 are overestimated whereas they are in excellent agreement with measurements for the two partially reticulated foams P2 and P3.

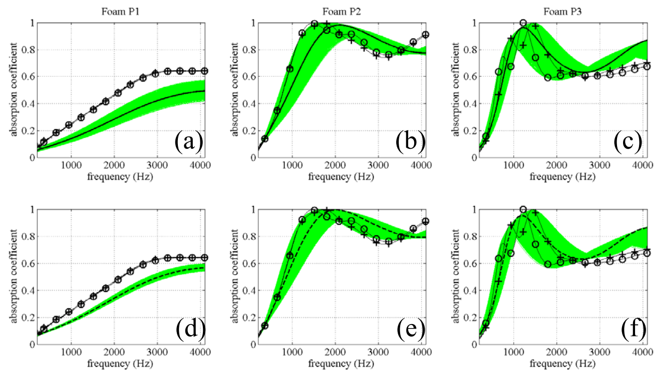


Figure 3: Sound absorption coefficient of 1 in. thick polyurethane foam layer: ((a),(d)) foam P1, ((b),(e)) foam P2, ((c),(f)) foam P3; (thick continuous line) model using the estimated non-acoustic properties from strut measurements; (thick discontinuous line) model using the estimated non-acoustic properties from cell size measurement; (green area) propagation of microstructure measurements uncertainties; (O,+) impedance tube measurements.

Overall good prediction is observed for three foams keeping in mind that the models use only microstructure measured parameters. Discrepancies observed for foam P1 can be attributed to the optical method chosen to determine the characteristic properties of the microstructure (struct thickness, length, cell size…). This is coherent with the conclusion of Perrot et al. [20] who couple direct measurements of porosity and airflow resistivity to 3D numerical computations to get the microstructure characteristic dimensions of the foam (PUC size). Discrepancies could also be attributed to the fact that SEM pictures for microstructure characterization have not been taken on the samples used for the acoustic characterization and thus stress the sensibility of the proposed semi-empirical method to the foam homogeneity. Nevertheless, despite its relative simplicity, the semi-empirical approach correctly estimates the sound absorption behavior of polyurethane foams being fully or partially reticulated as shown in Figure 3. Figs. 3 (d)-(f) validate the simplified model (two parameters model), which provides simulations closer to measurements with reduced uncertainties.

# 6 Conclusion

This paper presented a simplification and validation of the semi-empirical model recently proposed by the authors [1] to link the microstructure of PU foams with their sound absorbing behaviour. The initial model estimates the non-acoustic properties, involved in the Johnson-Champoux-Allard model, from cell shape consideration and measurements of microstructure properties such as strut length and thickness and reticulation rate. Scales factors specific to PU foams are given in this paper and provide a straightforward estimation of the non-acoustic properties of PU foams based only on cell size and reticulation rate measurements. The initial model was validated using 15 PU foams. The model and its simplification are validated in this paper using three new fully and partially reticulated PU foams. It is shown that the acoustic behaviour of the foams predicted from the Johnson-Champoux-Allard model using the non-acoustic properties estimated from the proposed semi-empirical model are in good agreement with impedance tube measurements.

# Acknowledgments

The authors would like to thank the National Sciences and Engineering Research Council of Canada (NSERC) for providing financial support.

# References

[1] O. Doutres, N. Atalla, K. Dong, “Effect of the microstructure closed pore content on the acoustic behavior of polyurethane foams”, *J. Appl. Phys.* 110**,** 064901 (2011)

[2] C. Perrot, R. Panneton, X. Olny, “Periodic unit cell reconstruction of porous media: Application to an open cell aluminum foam,” *J. Appl. Phys*. **101**, 113538 (2007)

[3] J.F. Allard and N. Atalla, *Propagation of sound in porous media: Modeling sound absorbing materials*, second edition, New York, Willey (2009)

[4] Y. Salissou, R. Panneton, “Pressure/mass method to measure open porosity of porous solids*”, J. Appl. Phys*. 101, 124913.1 (2007)

[5] M.R. Stinson, G.A. Daigle, “Electronic system for the measurement of flow resistance,” *J. Acoust. Soc. Am.* 83, 2422 (1988)

[6] M. Melon, B. Castagnede, “Correlation between tortuosity and transmission coefficient of porous media at high frequency,” *J. Acoust. Soc. Am.* 98, 1228 (1995)

[7] Z.E.A. Fellah, S. Berger, W. Lauriks, C. Depollier, C. Aristégui, J.-Y. Chapelon, “Measuring the porosity and the tortuosity of porous materials via reflected waves at oblique incidence”, *J. Acoust. Soc. Am.* 113(5), 2424 (2003)

[8] R. Panneton, X. Olny, “Acoustical determination of the parameters governing viscous dissipation in porous media”, *J. Acoust. Soc. Am.* 119(4), 2027 (2006)

[9] X. Olny, R. Panneton, “Acoustical determination of the parameters governing thermal dissipation in porous media”, *J. Acoust. Soc. Am.* 123(2), 814 (2008)

[10] Y. Salissou, R. Panneton, O. Doutres, “Complement to standard method for measuring normal incidence sound transmission loss with three microphones*”, J. Acoust. Soc. Am.* 131(3), EL 216 (2012)

[11] D. Lafarge, P. Lemarinier, J.-F. Allard, V. Tarnow, “Dynamic compressibility of air in porous structures at audible frequencies”, *J. Acoust. Soc. Am.* 102, 1995 (1997)

[12] L. J. Gibson, M.F. Ashby, *Cellular Solids—Structure and Properties*, second edition , Cambridge University Press, Cambridge (1997)

[13] P. Göransson, “Acoustic and vibrational damping in porous solids”, *Philosophical Transactions of the Royal Society A* 364, 89 (2006)

[14] E. Lind-Nordgren, P. Göransson, “Optimising open porous foam for acoustical and vibrational performance”, *J. Sound and Vib.* 329, 753 (2010)

[15] R.F. Lambert, “The acoustical structure of highly porous open-cell foams”, *J. Acoust. Soc. Am.* 72 (3), 879-887 (1982)

[16] I.P. Dunn IP, W.A. Davern, “Calculation of acoustic impedance of multi-layer absorbers”, *Appl. Acoust.* 19(5), 321–33 (1986)

[17] A. Cummings and SP. Beadle, “Acoustic properties of reticulated plastic foams”, *J. Sound and Vib.* 175(1), 115–133 (1993)

[18] J-P. Bonnet, F. Topin, L. Tadrist, “Flow laws in metal foams: compressibility and pore size effects”, *Transp. Porous Med.* 73, 233-254 (2008)

[19] Anonymous, “Acoustics - Determination of sound absorption coefficient and impedance in impedance tubes. Part 2: Transfer-function method,” *International Standard ISO-10534-2* (1998)

[20] C. Perrot, F. Chevillotte, M.-T. Hoang, G. Bonnet, F.-X. Bécot, L. Gautron, A. Duval, “Microstructure, transport, and acoustic properties of open-cell foam samples: Experiments and three-dimensional numerical simulations”, *J. Appl. Phys*. **111**, 014911 (2012)